Author Manuscript

Author Manuscript

Author Manuscript

Author Manuscript

HHS Public Access

Author manuscript

JAMA Facial Plast Surg. Author manuscript; available in PMC 2015 September 01.

Published in final edited form as:

JAMA Facial Plast Surg. 2014 ; 16(5): 319–327. doi:10.1001/jamafacial.2014.395.

Characterization of Postoperative Changes in Nasal Airflow Using a Cadaveric Computational Fluid Dynamics Model:

Supporting the Internal Nasal Valve

Scott Shadfar, MD, **William W. Shockley, MD**, **Gita M. Fleischman, MD**, **Anand R. Dugar, MD**, **Kibwei A. McKinney, MD**, **Dennis O. Frank-Ito, PhD**, and **Julia S. Kimbell, PhD**

Meridian Plastic Surgeons, Indianapolis, Indiana (Shadfar); Department of Otolaryngology–Head and Neck Surgery, University of North Carolina, Chapel Hill (Shockley, Fleischman, Dugar, McKinney, Kimbell); Division of Otolaryngology–Head and Neck Surgery, Duke University Medical Center, Durham, North Carolina (Frank-Ito)

Abstract

IMPORTANCE—Collapse or compromise of the internal nasal valve (INV) results in symptomatic nasal obstruction; thus, various surgical maneuvers are designed to support the INV.

OBJECTIVE—To determine the effect on nasal airflow after various surgical techniques focused at the level of the INV and lateral nasal sidewall.

DESIGN AND SETTING—A fresh cadaver head was obtained and underwent suture and cartilage graft techniques directed at the level of the INV using an external approach. Preoperative and postoperative digital nasal models were created from the high-resolution, fine-cut, computed tomographic imaging after each intervention. Isolating the interventions to the level of the INV, we used computational fluid dynamic techniques to calculate nasal resistance, nasal airflow, and nasal airflow partitioning for each intervention.

INTERVENTION—Suture and cartilage graft techniques.

MAIN OUTCOMES AND MEASURES—Nasal airflow, nasal resistance, and partitioning of airflow.

Copyright 2014 American Medical Association. All rights reserved.

Corresponding Author: Julia S. Kimbell, PhD, Department of Otolaryngology–Head and Neck Surgery, University of North Carolina, Chapel Hill, 170 Manning Dr, Campus Box 7070, Chapel Hill, NC 27599-7070 (julia_kimbell@med.unc.edu).

Conflict of Interest Disclosures: None reported.

Author Contributions: Dr Shadfar had full access to all the data in the study and takes responsibility for the integrity of the data and the accuracy of the data analysis.

Study concept and design: Shadfar, Shockley, Fleischman, McKinney, Frank-Ito, Kimbell.

Acquisition, analysis, or interpretation of data: Shadfar, Fleischman, Dugar, McKinney, Frank-Ito, Kimbell.

Drafting of the manuscript: Shadfar, Shockley, Fleischman, Dugar.

Critical revision of the manuscript for important intellectual content: Shadfar, Shockley, Fleischman, McKinney, Frank-Ito, Kimbell.

Statistical analysis: Shadfar, Fleischman, Dugar.

Obtained funding: Fleischman.

Administrative, technical, and material support: Shadfar, Shockley, Fleischman, McKinney, Frank-Ito, Kimbell.

Study supervision: Shockley, Kimbell.

Role of the Sponsor: The funding source had no role in the design and conduct of the study; collection, management, analysis, and interpretation of the data; preparation, review, or approval of the manuscript; and decision to submit the manuscript for publication.

Author Manuscript Author Manuscript Author Manuscript Author Manuscript

RESULTS—Using the soft-tissue elevation model as baseline, computational fluid dynamic analysis predicted that most of the suture and cartilage graft techniques directed toward the nasal valve improved nasal airflow and partitioning while reducing nasal resistance. Specifically, medial and modified flare suture techniques alone improved nasal airflow by 16.9% and 15.1%, respectively. The combination of spreader grafts and modified flare suture improved nasal airflow by 13.2%, whereas spreader grafts alone only improved airflow by 5.9%. The largest improvements in bilateral nasal resistance were achieved using the medial and modified flare sutures, outperforming the combination of spreader grafts and modified flare suture.

CONCLUSIONS AND RELEVANCE—Techniques directed at supporting the INV have tremendous value in the treatment of nasal obstruction. The use of flare sutures alone can address dynamic valve collapse or upper lateral cartilage incompetence without gross disruption of the nasal architecture. Using computational fluid dynamic techniques, this study suggests that flare sutures alone may improve flow and reduce resistance when placed medially, surpassing spreader grafts alone or in combination with flare sutures. The longevity of these maneuvers can only be assessed in the clinical setting. Studies in additional specimens and clinical correlation in human subjects deserve further attention and investigation.

LEVEL OF EVIDENCE—NA.

The internal nasal valve (INV) encompasses the area between the head of the inferior turbinate, caudal edge of the upper lateral cartilage (ULC), nasal floor, and cartilaginous septum. The INV is the segment of the nasal air way with the highest resistance to flow. Based on the Bernoulli principle, acceleration of flow in an area of high resistance leads to a drop in intraluminal pressure, increasing the potential for nasal valve compromise (NVC) in a potentially already weakened segment.[1] Anatomical nasal deformities within this region, whether congenital, traumatic, idiopathic, or iatrogenic, can lead to symptomatic nasal obstruction. In addition, compensatory and inflammatory changes can induce inferior turbinate hypertrophy and further obstruct the nasal airway.

Recently, a panel convened by the American Academy of Otolaryngology–Head and Neck Surgery released a clinical consensus statement on the diagnosis and management of NVC.[2] The consensus panel agreed that NVC is best evaluated with history and physical examination findings; although management can include medical therapies, surgical management is the mainstay for treatment of anatomical nasal deformities leading to NVC. A 25-year review by Rhee and colleagues[3] concluded that evidence supported the efficacy of modern-day rhinoplasty techniques for treatment of nasal obstruction secondary to NVC. The evolution of NVC as a clinical entity has sparked a multitude of techniques directed at addressing NVC. Nasal valve repair, often synonymous with functional rhinoplasty, uses techniques such as spreader grafts, flaring and suspension sutures, and butterfly and alar batten grafts, all designed to correct or strengthen the nasal valve and middle cartilaginous vault.[4–8] However, how these techniques, individually or in combination, compare in objectively reducing nasal obstruction is not clear, and the emphasis recently has been placed on incorporating objective measures or validated patient-reported outcome measures into new and existing studies.[9–13]

Author Manuscript Author Manuscript Author Manuscript Author Manuscript

A variety of objective measurements, including physical examination findings, rhinomanometry, and acoustic rhinometry, have been used in the past to evaluate nasal airway obstruction (NAO). Unfortunately, besides the physical examination, past objective measurements of nasal function and airflow did not always correlate with patient-reported symptoms, posing severe limitations in their use.[14,15] With the emergence of anatomically accurate 3-dimensional (3D) computational models generated from computed tomography (CT) or magnetic resonance imaging data, some of the multifactorial causes of NAO and NVC can be dissected into individual components. Computational fluid dynamics (CFD) is a technique that can be used to study nasal airflow and resistance in 3D models and other aspects of nasal physiology (eg, humidification, heatex change, and olfaction).[16–18] Early reports[19,20] have begun to establish a correlation of objective CFD analyses with patient-reported symptoms, further validating its diagnostic utility in NVC. Moreover, 3D computational models provide potential for planning and analysis with the ability to simulate surgical changes preoperatively using virtual models. The virtual models could then be evaluated using CFD techniques to predict changes in nasal airflow and resistance that will most likely result in the desired outcome and improvement.[21,22]

The focus of the present study was to provide a direct objective comparison of maneuvers addressing NVC, specifically isolated to the level of the INV at the ULC and middle cartilaginous vault. We compared CFD-derived quantities, including nasal resistance, nasal airflow, and inspiratory airflow, by partitioning before and after 6 individual and combination surgical procedures in the same cadaver.

Methods

Cadaver Dissections

A single fresh cadaver head (Life Science Anatomical) was cleansed and irrigated to remove any clots and debris from the nasal cavities. The head was dissected beginning with cartilage harvest posterior to the internal valve region using a right-sided hemitransfixion incision, which was then closed in a standard fashion. Bony septal deviation was not present, and this portion of the dissection only served as a source of cartilage for grafting purposes. Next, using marginal and transcolumellar incisions, we took an external rhinoplasty approach, elevating the soft-tissue envelope deep to the superficial musculoaponeurotic system and to the level of the nasal bones. We closed the incisions and obtained modified contiguous CT scans in the axial plane of the entire nasal cavity and external nasal soft tissue (0.425-mm increments). After each of the following interventions, this process was repeated with redraping of the soft-tissue envelope and suture placement, followed by CT imaging. For the purpose of our categorizations, we choose the following suture terms: classic or lateral flare, medial flare, and modified flare. We use the terms *flaring suture* and *flare suture* interchangeably. Other grafting techniques, such as batten or butterfly grafts, were not performed.

Lateral Flare Suture

The 5 interventions tested started with placement of the lateral or classic flaring suture[5] beginning 6 mm from the mid-line at the level of the caudal aspect of the ULC junction with

Author Manuscript Author Manuscript Author Manuscript Author Manuscript

the lower lateral cartilage. Using a 4-0 polypropylene suture on a taper needle (RB-1; Ethicon, Inc), we traveled 4 to 5 mm (following the natural curvature of the needle) directly vertical and ending 6 mm lateral to the midline septum at the cephalic aspect of the suture pass. The suture was then crossed to the contralateral side and performed in an identical fashion 6 mm lateral to the midline at the cephalic and caudal aspects of the suture, forming a rectangular shape with the suture as it was tied (Figure 1A).

Modified Flare Suture

Next, we removed the previous suture and performed the modified flare suture beginning 6 mm from the midline at the level of the caudal aspect of the ULC junction with lower lateral cartilage. Using a 4-0 polypropylene suture on an RB-1 needle, we traveled approximately 5 mm (following the natural curvature of the needle) diagonally toward the midline, ending 4 mm lateral to the midline septum at the cephalic aspect of the suture pass. The suture was then crossed to the contralateral side and performed in an identical fashion 4 mm lateral to the midline at the cephalic aspect and 6 mm at the caudal aspect of the suture, forming a trapezoid shape with the suture as it was tied (Figure 1B).

Medial Flare Suture

Next, we removed all sutures and placed the medial flare suture beginning 4 mm from the midline at the level of the caudal aspect of the ULC junction with lower lateral cartilage. Using a 4-0 polypropylene suture on an RB-1 needle, we traveled 4 to 5 mm (following the natural curvature of the needle) in a direct vertical path ending 4 mm lateral to the midline septum at the cephalic aspect of the suture pass. The suture was then crossed to the contralateral side and performed in an identical fashion 4 mm lateral to the midline at the cephalic and caudal aspects of the suture, forming a square shape with the suture as it was tied (Figure 1C).

Spreader Grafts

We then fashioned bilateral spreader grafts from the harvested cartilage measuring 1.5 mm in width and 4 mm in height and extended from the caudal aspect of the nasal bones through the entire length of the released ULCs. These grafts were sewn into place using horizontal mattress 5-0 polydioxanone sutures along the course of the grafts, incorporating the ULCs and reconstituting them.

Spreader Graft With Modified Flare Suture

The final technique combined bilateral spreader grafts with the modified flare suture. The soft-tissue envelope was raised, and a modified flare suture technique identical to that described above was used with the spreader grafts already in place, combining the 2 interventions. The soft-tissue envelope was redraped and sutured closed, followed by CT imaging.

Modeling and Simulations

The cadaver head underwent imaging after each surgical intervention, which yielded 6 separate CT scans (soft-tissue envelope alone, lateral flare suture, modified flare suture,

Author Manuscript Author Manuscript Author Manuscript Author Manuscript

medial flare suture, spreader grafts, and spreader grafts with modified flare suture) using the Digital Imaging and Communication in Medicine file format (http://medical.nema.org). Each scan was imported into medical imaging software (Mimics, version 14.01; Materialise, Inc). For each of the 6 interventions studied, an anatomically accurate 3D reconstruction of the nasal airspace was generated by selecting pixels with a maximum of −315 H to represent the sinonasal airspace. The soft-tissue elevation (STE) model was used as the reference to which all other reconstructions were coregistered, with the facial bones as points of reference.

To isolate the effect of each intervention and to minimize tissue decay artifacts, 5 hybrid reconstructions were created by combining anterior and posterior valve segments of the STE model with a coregistered wedge-shaped segment containing the INV from each of the other 5 reconstructions (lateral, modified, and medial flare, spreader grafts, and spreader grafts plus modified flare suture) (Figure 2). The 5 hybrid reconstructions and the STE reconstruction were then exported in stereolithography file format to meshing and computer-aided design software (ICEM-CFD, version 14.0; ANSYS), in which we created planar surfaces at the nostrils and outlet for airflow boundary conditions and computational meshes of the nasal airspace. Each computational mesh consisted of approximately 4 million unstructured, graded, tetrahedral elements.

Next, we conducted airflow simulations using CFD software (Fluent, version 14.0; ANSYS, Inc). Steady-state, laminar, inspiratory airflow was simulated under pressure-driven conditions similar to those described by Frank et al.[23] At the nostrils, a pressure-inlet boundary type was used with static pressure set to 0 Pa. A pressure-outlet boundary type was used at the nasopharynx, with the gauge pressure set to −10 Pa.

The simulations were visualized and analyzed using the CFD software and postprocessing software (FieldView, version 13.0; Intelligent Light). Laterality of volumetric airflow partitioning (percentage of total flow) and bilateral and unilateral nasal resistance (in pascals per milliliter per second) were calculated, with nasal resistance equal to the drop in bilateral or unilateral area-weighted mean pressure from the nostrils to the posterior end of the nasal septum divided by the bilateral or unilateral flow rate (in liters per minute), respectively. Comparison calculations were performed with the STE simulation serving as baseline.

Results

Nasal Airflow

Nasal airflow is defined as the volume of air inspired over a defined time. All maneuvers had a positive effect on nasal airflow when compared with the flow within the STE model. The largest increases in bilateral nasal airflow were seen with the medial and modified flare sutures, with 16.9% and 15.1% increases, respectively. The spreader graft and flare suture combination allowed a 13.2% gain in bilateral airflow. The lateral flare suture provided a 10.0% increase in airflow, while the spreader graft alone afforded a modest 5.9% increase (Table 1).

Author Manuscript Author Manuscript Author Manuscript Author Manuscript

Airflow Partitioning

Airflow partitioning refers to the percentage of airflow passing through right and left nasal cavities in comparison with the total nasal cavity. Partitioning of airflow between the nasal cavities was also altered by the interventions (Table 2). After the STE and cartilage harvest, 66.7% of airflow passed through the right side of the nose, and 33.3% passed through the left side. The combination spreader graft and flare suture provided the most balanced partitioning pattern with 53.9% of airflow passing through the right side and 46.1% through the left side. The medial and modified flare sutures also improved the partitioning similarly (Table 2). The isolated spreader graft model provided only a modest improvement in partitioning with only a 6.3% improvement toward an even allocation. The lateral flare suture provided less than all other flare sutures with an 8.3% improvement in partitioning.

Nasal Resistance

Nasal resistance measures the access of inspired air into the nasal cavity. After cartilage harvest and STE, the bilateral nasal resistance was 0.0205 Pa/(mL/s), and unilateral right and left nasal resistances were 0.0305 and 0.0619 Pa/(mL/s), respectively. The largest reductions in bilateral nasal resistance were achieved using the medial and modified flare sutures, with improvements in resistance by 12.7% and 10.7% respectively (Table 3). These flare sutures slightly outperformed the combination of spreader grafts and modified flare suture, which reduced bilateral resistance by 9.3%. The classic or laterally based flare suture reduced bilateral resistance by only 3.4%. Conversely, we found evidence of an increase in bilateral nasal resistance of 2.4% with spreader grafts alone.

Left-sided unilateral resistance measurements showed the largest reductions from the STE state with the spreader graft and modified flare suture combination, followed by the medial and modified flare sutures, with 34.4%, 32.8%, and 32.0% reductions, respectively (Table 4). The lateral flare suture decreased STE left-sided resistance by 22.5%. Because increases in left-sided airflow were mirrored by right-sided decreases, right nasal cavity unilateral resistances increased with all the techniques, with the spreader graft model showing the greatest rise in resistance with a 13.1% change from the STE right-sided resistance (Table 4). The combination of the modified flare suture and spreader graft showed a large 11.8% increase in resistance on the right side. The lateral flare suture increased right-sided resistance by 10.2% compared with STE. The medial and modified flare sutures had the smallest increases in resistance on the right side, with changes from STE of only 2.3% and 5.6%, respectively.

Discussion

Surgical correction of NVC has garnered a significant amount of attention in nasal surgery with raised awareness of the toll NVC can have on a patient's quality of life.[12,24] This attention has prompted an evolution in surgical maneuvers for treating NVC, with a new emphasis on outcome measures, given the unacceptable rates of failure ranging up to 35%.[25–29] These excessive rates of continued symptoms could be attributed to multilevel obstruction, failure to address all anatomical deformities, and weak correlations between patient-reported symptoms with the already insufficient quantitative methods

Author Manuscript Author Manuscript Author Manuscript Author Manuscript

available.[14,30,31] This constellation of causes has set the stage for CFD modeling and simulations to come into the forefront of analyses focusing on the effects that common abnormalities and surgical changes can have on nasal airflow.[19,21,22,32–36] The correlation of CFD-derived variables with patient-reported data are under evaluation, with early reports showing CFD as a potential validated method.[19,20] A significant benefit of CFD over other objective measures was the ability to calculate variables precisely and directly at the INV, addressing form and function simultaneously.

A prospective study using rhinomanometry performed by Constantian and Clardy[37] evaluated NAO stratified by the site of the obstruction. They included evaluations of septal deviation, external nasal valve, and INV and excluded inferior turbinate hypertrophy. The postoperative results showed that the effects of nasal valve collapse may equal or even exceed septal deviation as the principal cause of NAO. This finding led to other studies evaluating various techniques, including spreader grafts, flaring and suspension sutures, and butterfly and alar batten grafts.[4–8,38] The limitations in most of these earlier studies were related to difficulties in determining the exact anatomical site of obstruction because the outcomes were based on subjective data or acoustic rhinometry and rhinomanometry. In addition, rhinometry and rhinomanometry can be inaccurate when measuring INV cross-sectional area and often require measurements to be taken at higher airflow rates.[3,14] In comparison, CFD allows measurement of unilateral resistance at lower airflow rates approximating resting breathing rates, with precise anatomical detail.[19] The objective data collected with acoustic rhinometry include INV minimal cross-sectional area, nasal resistance, and nasal volume; however, acoustic rhinometry does not allow determination of the type of airflow (laminar, transitional, or turbulent), partitioning, humidification, heat flux, or wall shear stress. These additional measurements potentially serve as surrogates for patient-reported improvement as opposed to minimal cross-sectional areas at the level of the INV.[20,39]

As described above, several CFD studies[19,21,22,32–36] have evaluated the treatment of NAO with septoplasty and/or inferior turbinate reduction with conclusions that the septum and turbinate are major contributors in NAO, but most did not investigate the influence of the ULC or lateral nasal sidewall in isolation. One recent study[22] used CFD analysis and virtual models in a single patient who underwent combined nasal valve repair, septoplasty, and turbinate reduction operations and concluded that nasal valve repair may have had less effect than the septoplasty and turbinate reductions. However, that study focused on a single patient in whom true isolation of the nasal valve repair surgery alone was not possible. To our knowledge, the present study is the first description of the effects of isolated surgical maneuvers directed at the INV and ULC using CFD analysis.

Using STE as our baseline model allowed uniform comparisons of the nasal airway models after disruption of the support mechanisms that may have been in place before the STE and any influence that may have been observed secondary to the cartilage harvest. Specific technical details about the exact placement of the conventional flaring suture are not available in the literature. As a result, surgical judgment typically dictates suture placement. The positioning of our lateral or classic flare suture was based on the diagrams and descriptions written by Park,[5] the first study to describe the use of a flaring suture for

Author Manuscript Author Manuscript Author Manuscript Author Manuscript

treatment of NVC and NAO. Within the following year, Schlosser and Park[38] used acoustic rhinometry to evaluate the influence of spreader grafts, flaring sutures, and batten grafts on a minimal cross-sectional area of the INV in cadavers. They found that the combination of spreader grafts and flaring sutures had the greatest effect on the cross-sectional area of the INV. Within our analysis, the same lateral flare suture described previously had the least effect on nasal airflow, resistance, and redistribution of airflow compared with all other flare suture positions. However, the lateral flare suture had marginally improved dynamics compared with the isolated use of spreader grafts, which was the poorest overall performer. This latter comparison is similar to what Schlosser and Park[38] published when comparing the flare suture and the spreader graft; Zoumalan and Constantinides[40] had similar findings. Our combination of the spreader graft with flare suture had a more dramatic effect on all tested variables compared with the lateral flare suture or spreader graft method used alone. However, the combination technique was not consistently the superior maneuver in contradistinction to what others have previously published.

The use of spreader grafts most often involves the release of the ULC from the cartilaginous septum and dissection of a mucoperichondrial pocket to allow appropriate positioning. Frequently, as in our dissection, the ULC is reconstituted to avoid midvault collapse. The width of spreader grafts can be varied to achieve improved aesthetic and functional benefit. Our examination was limited to a single graft on each side, keeping the width constant among models. Increasing the width of the spreader grafts by using double- or triple-stacked grafts could have had an effect on the airflow analysis, although the balance between function and an aesthetically wide nose should be kept in mind. Clinically, the failures seen with spreader grafts are often nuances associated with destabilization of the ULC (middle vault) during release, graft positioning, or the size of the graft. When fashioning spreader grafts, the height should be maintained from 3 to 6 mm to avoid a counterproductive effect on flow and resistance by impinging on the airway.[41]

Although all the above-mentioned precautions were taken in our dissection, the spreader graft alone carried the highest increase in unilateral nasal resistance, with a 13.1% increase on the right side. The spreader graft was the only technique to result in increased, although minor, bilateral nasal resistance. The combination of spreader graft and modified flare suture offered the largest decrease in left-sided unilateral resistance; however, we also found an 11.8% increase in contralateral resistance. This increase resulted in a lower percentage of improvement in bilateral nasal resistance with the spreader graft and modified flare suture combination, likely owing to the negative effect of the spreader grafts on nasal flow and associated pressure changes (Figure 3). We believe that most of the positive effects seen on resistance and partitioning from the combination technique came from the modified flare as opposed to the spreader graft based on the individual patterns of resistance and partitioning for each maneuver.

We further evaluated permutations in the position of the flare suture to determine the ideal location to maximize nasal airflow dynamics (Figure 1). The placement of the medial and modified flare sutures was designed specifically to isolate the nasal valve without pinching or bunching of the ULC, which can sometimes be seen with the classic lateral flare suture. A more medially positioned flare suture proved beneficial, exhibiting the largest increases in

Author Manuscript Author Manuscript Author Manuscript Author Manuscript

flow and the most significant reduction in bilateral resistance. When compared with the medial flare suture, the modified flare suture offered comparable increases in flow and decreases in unilateral and bilateral resistance and even surpassed the medial flare suture in airflow partitioning. These 2 sutures shared a common cephalic point at 4 mm lateral to the mid-line, approximately 5 mm from the scroll (Figure 4). This shared area of augmentation may serve as a critical region in valve patency and could explain why the performance of these 2 sutures was superior, but this possibility deserves further investigation.

Computational fluid dynamics models can be used to investigate nasal airflow, and the exact variables that correlate between surgical interventions and patient symptoms are more likely to be multifactorial, such as a combination of nasal airflow, resistance, partitioning, or heat flux.[20] Based on Tables 1 through 4, the medial flare was consistently the most effective intervention, with the modified flare following as a close second.

Although the combination of the spreader graft and modified flare surpassed the other interventions in a select few variables, taken as a whole, the isolated flare sutures had more consistent improvements without disruption of the underlying nasal architecture. Considering isolated suturing techniques as the superior intervention in nasal valve reconstruction infringes on the dogma of most nasal surgeons who rely on grafting techniques for treating valvular collapse. Our findings may substantiate transformation and discussion because precisely positioned flare sutures might decrease the morbidity associated with septal or conchal cartilage harvest by avoiding grafting techniques. In addition, reduced operative times could be seen with flare suture placement compared with complex grafting, which requires cartilage harvesting, shaping, and positioning. Also, flare sutures could be ideal in the patient population with multiple revisions and presenting with valvular collapse, given that most of these patients often have a paucity of autologous material. Although these concepts are preliminary at this stage and long-term studies are needed to determine the longevity of flare sutures, flaring sutures appear to play a greater role in the treatment of NVC and NAO.

Limitations in our study include the dissections being performed on a single cadaver specimen. Although fresh, the specimen lacked the resiliency of living tissue, and current modeling practices did not account for dynamic collapse. In addition, the changes encountered from postoperative edema or fibrosis could not be taken into account, which can also have an effect on long-term subjective and objective measures in patients. The long-term beneficial effects of any suture technique can only be speculated. Only 1 cadaver head was used secondary to the laborious nature of 3D reconstruction and CFD analysis as outlined in the Methods section, which prohibited statistical analysis. The focus of our study was also limited to flaring sutures and spreader grafts; however, other grafting techniques, such as butterfly and batten grafts, could be examined in future studies. We believed that the use of a hybrid model allowed us to isolate the nasal valve area by keeping the dynamic nasopharynx and nostril segments constant. Using a cadaveric model prevented nasal cycling from having any influence between preoperative and postoperative imaging, which can often be a confounder in CFD modeling.

Author Manuscript Author Manuscript Author Manuscript Author Manuscript

Conclusions

Computational fluid dynamics analysis examining the exact position of flare sutures has not been published before our study. Our preliminary cadaveric data suggest that medially positioned flare sutures may clinically outperform spreader grafts alone or in combination with flare sutures, with minimal to no disruption or weakening of the underlying nasal architecture. Future studies using additional specimens and living subjects are needed for comparison, with attention directed to subjective and objective data correlation using Nasal Obstruction Symptom Evaluation scores[9] and CFD measures, such as nasal resistance and heat flux, in combination with the flare suture.

Acknowledgments

Funding/Support: This study was supported by National Research Service Award Institutional Training Grant 5T32DC005360 from the National Institutes of Health (University of North Carolina).

References

1. Ishii LE, Rhee JS. Are diagnostic tests useful for nasal valve compromise? Laryngoscope. 2013; 123 (1):7–8. [PubMed: 23280938]
2. Rhee JS, Weaver EM, Park SS, et al. Clinical consensus statement: diagnosis and management of nasal valve compromise. Otolaryngol Head Neck Surg. 2010; 143(1):48–59. [PubMed: 20620619]
3. Rhee JS, Arganbright JM, McMullin BT, Hannley M. Evidence supporting functional rhinoplasty or nasal valve repair: a 25-year systematic review. Otolaryngol Head Neck Surg. 2008; 139(1):10–20. [PubMed: 18585555]
4. Sheen JH. Spreader graft: a method of reconstructing the roof of the middle nasal vault following rhinoplasty. Plast Reconstr Surg. 1984; 73 (2):230–239. [PubMed: 6695022]
5. Park SS. The flaring suture to augment the repair of the dysfunctional nasal valve. Plast Reconstr Surg. 1998; 101(4):1120–1122. [PubMed: 9514349]
6. Friedman M, Ibrahim H, Syed Z. Nasal valve suspension: an improved, simplified technique for nasal valve collapse. Laryngoscope. 2003; 113(2):381–385. [PubMed: 12567100]
7. Clark JM, Cook TA. The “butterfly” graft in functional secondary rhinoplasty. Laryngoscope. 2002; 112(11):1917–1925. [PubMed: 12439155]
8. Tardy ME, Garner ET. Inspiratory nasal obstruction secondary to alar and nasal valve collapse: technique for repair using autologous cartilage. Oper Tech Otolaryngol Head Neck Surg. 1990; 1(3):215–218.
9. Stewart MG, Witsell DL, Smith TL, Weaver EM, Yueh B, Hannley MT. Development and validation of the Nasal Obstruction Symptom Evaluation (NOSE) scale. Otolaryngol Head Neck Surg. 2004; 130(2):157–163. [PubMed: 14990910]
10. Most SP. Analysis of outcomes after functional rhinoplasty using a disease-specific quality-of-life instrument. Arch Facial Plast Surg. 2006; 8(5):306–309. [PubMed: 16982985]
11. Stewart MG, Smith TL, Weaver EM, et al. Outcomes after nasal septoplasty: results from the Nasal Obstruction Septoplasty Effectiveness (NOSE) Study. Otolaryngol Head Neck Surg. 2004; 130(3):283–290. [PubMed: 15054368]
12. Rhee JS, Poetker DM, Smith TL, Bustillo A, Burzynski M, Davis RE. Nasal valve surgery improves disease-specific quality of life. Laryngoscope. 2005; 115(3):437–440. [PubMed: 15744153]
13. Lang C, Grützenmacher S, Mlynski B, Plontke S, Mlynski G. Investigating the nasal cycle using endoscopy, rhinoresistometry, and acoustic rhinometry. Laryngoscope. 2003; 113(2):284–289. [PubMed: 12567083]

Author Manuscript Author Manuscript Author Manuscript Author Manuscript

14. Pawar SS, Garcia GJ, Kimbell JS, Rhee JS. Objective measures in aesthetic and functional nasal surgery: perspectives on nasal form and function. Facial Plast Surg. 2010; 26(4):320–327. [PubMed: 20665410]
15. Chandra RK, Patadia MO, Raviv J. Diagnosis of nasal airway obstruction. Otolaryngol Clin North Am. 2009; 42(2):207–225. vii. [PubMed: 19328887]
16. Garcia GJ, Bailie N, Martins DA, Kimbell JS. Atrophic rhinitis: a CFD study of air conditioning in the nasal cavity. J Appl Physiol. 2007; 103(3):1082–1092. [PubMed: 17569762]
17. Lindemann J, Keck T, Wiesmiller K, et al. A numerical simulation of intranasal air temperature during inspiration. Laryngoscope. 2004; 114(6):1037–1041. [PubMed: 15179209]
18. Zhao K, Scherer PW, Hajiloo SA, Dalton P. Effect of anatomy on human nasal air flow and odorant transport patterns: implications for olfaction. Chem Senses. 2004; 29(5):365–379. [PubMed: 15201204]
19. Kimbell JS, Garcia GJ, Frank DO, Cannon DE, Pawar SS, Rhee JS. Computed nasal resistance compared with patient-reported symptoms in surgically treated nasal airway passages: a preliminary report. Am J Rhinol Allergy. 2012; 26 (3):e94–e98.10.2500/ajra.2012.26.3766 [PubMed: 22643935]
20. Kimbell JS, Frank DO, Laud P, Garcia GJ, Rhee JS. Changes in nasal airflow and heat transfer correlate with symptom improvement after surgery for nasal obstruction. J Biomech. 2013; 46(15): 2634–2643. [PubMed: 24063885]
21. Rhee JS, Pawar SS, Garcia GJ, Kimbell JS. Toward personalized nasal surgery using computational fluid dynamics. Arch Facial Plast Surg. 2011; 13(5):305–310. [PubMed: 21502467]
22. Rhee JS, Cannon DE, Frank DO, Kimbell JS. Role of virtual surgery in preoperative planning: assessing the individual components of functional nasal airway surgery. Arch Facial Plast Surg. 2012; 14 (5):354–359. [PubMed: 22508896]
23. Frank DO, Kimbell JS, Cannon D, Rhee JS. Computed intranasal spray penetration: comparisons before and after nasal surgery. Int Forum Allergy Rhinol. 2013; 3(1):48–55. [PubMed: 22927179]
24. Rhee JS, Book DT, Burzynski M, Smith TL. Quality of life assessment in nasal airway obstruction. Laryngoscope. 2003; 113(7):1118–1122. [PubMed: 12838007]
25. Singh A, Patel N, Kenyon G, Donaldson G. Is there objective evidence that septal surgery improves nasal airflow? J Laryngol Otol. 2006; 120 (11):916–920. [PubMed: 17040608]
26. Illum P. Septoplasty and compensatory inferior turbinate hypertrophy: long-term results after randomized turbinoplasty. Eur Arch Otorhinolaryngol. 1997; 254(suppl 1):S89–S92. [PubMed: 9065637]
27. André RF, D'Souza AR, Kunst HP, Vuyk HD. Sub-alar batten grafts as treatment for nasal valve incompetence: description of technique and functional evaluation. Rhinology. 2006; 44(2):118–122. [PubMed: 16792170]
28. Dinis PB, Haider H. Septoplasty: long-term evaluation of results. Am J Otolaryngol. 2002; 23(2): 85–90. [PubMed: 11893975]
29. Cannon DE, Rhee JS. Evidence-based practice: functional rhinoplasty. Otolaryngol Clin North Am. 2012; 45(5):1033–1043. [PubMed: 22980683]
30. Schumacher MJ. Nasal congestion and airway obstruction: the validity of available objective and subjective measures. Curr Allergy Asthma Rep. 2002; 2(3):245–251. [PubMed: 11918867]
31. Lam DJ, James KT, Weaver EM. Comparison of anatomic, physiological, and subjective measures of the nasal airway. Am J Rhinol. 2006; 20(5):463–470. [PubMed: 17063739]
32. Chen XB, Lee HP, Chong VF, Wang Y. Numerical simulation of the effects of inferior turbinate surgery on nasal airway heating capacity. Am J Rhinol Allergy. 2010; 24(5):e118–e122.10.2500/ajra.2010.24.3511 [PubMed: 21244728]
33. Garcia GJ, Rhee JS, Senior BA, Kimbell JS. Septal deviation and nasal resistance: an investigation using virtual surgery and computational fluid dynamics. Am J Rhinol Allergy. 2010; 24(1):e46–e53.10.2500/ajra.2010.24.3428 [PubMed: 20109325]
34. Wexler D, Segal R, Kimbell J. Aerodynamic effects of inferior turbinate reduction: computational fluid dynamics simulation. Arch Otolaryngol Head Neck Surg. 2005; 131(12):1102–1107. [PubMed: 16365225]

Author Manuscript Author Manuscript Author Manuscript Author Manuscript

35. Ozlugedik S, Nakiboglu G, Sert C, et al. Numerical study of the aerodynamic effects of septoplasty and partial lateral turbinectomy. Laryngoscope. 2008; 118(2):330–334. [PubMed: 18030167]
36. Lee HP, Poh HJ, Chong FH, Wang Y. Changes of airflow pattern in inferior turbinate hypertrophy: a computational fluid dynamics model. Am J Rhinol Allergy. 2009; 23(2):153–158. [PubMed: 19401040]
37. Constantian MB, Clardy RB. The relative importance of septal and nasal valvular surgery in correcting airway obstruction in primary and secondary rhinoplasty. Plast Reconstr Surg. 1996; 98 (1):38–58. [PubMed: 8657787]
38. Schlosser RJ, Park SS. Surgery for the dysfunctional nasal valve: cadaveric analysis and clinical outcomes. Arch Facial Plast Surg. 1999; 1(2):105–110. [PubMed: 10937087]
39. Zhao K, Jiang J, Blacker K, et al. Regional peak mucosal cooling predicts the perception of nasal patency. Laryngoscope. 2014; 124(3):589–595. [PubMed: 23775640]
40. Zoumalan RA, Constantinides M. Subjective and objective improvement in breathing after rhinoplasty. Arch Facial Plast Surg. 2012; 14(6):423–428. [PubMed: 22965002]
41. Toriumi D. Management of the middle nasal vault in rhinoplasty. Operat Tech Plast Reconstr Surg. 1995; 2(1):16–30.

Author Manuscript Author Manuscript Author Manuscript Author Manuscript

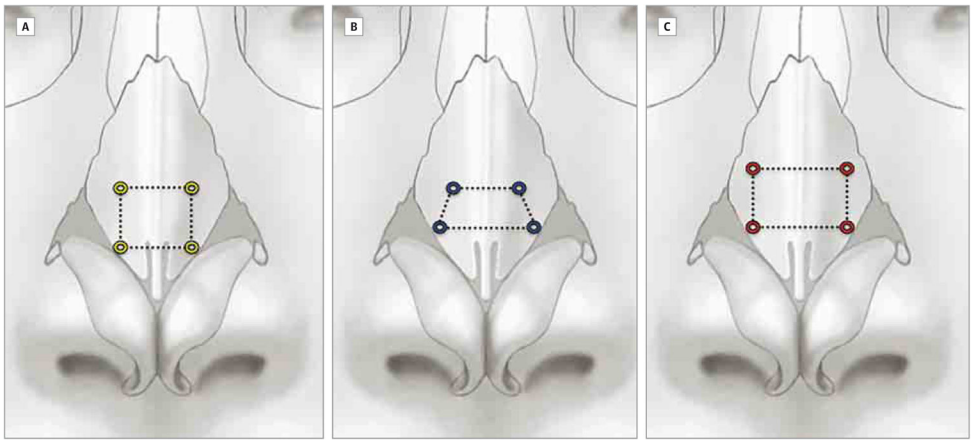

Figure 1.

Relationship of the Surgical Placement of the Flare Sutures

A, Medial (yellow square). B, Modified (blue trapezoid). C, Lateral (red rectangle).

Author Manuscript Author Manuscript Author Manuscript Author Manuscript

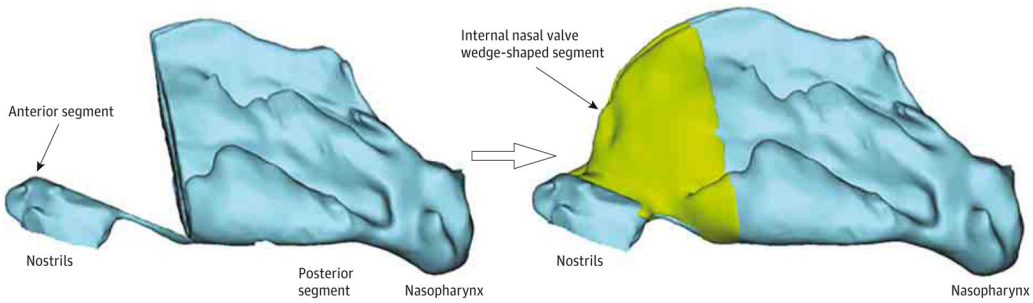

Figure 2.

Three-Dimensional Hybrid Reconstruction of the Soft-Tissue Elevation (STE) Model

We combined the anterior and posterior segments of the STE model (left) with a wedge-shaped segment containing the internal nasal valve from each of the other 5 reconstructions (right).

Author Manuscript Author Manuscript Author Manuscript Author Manuscript

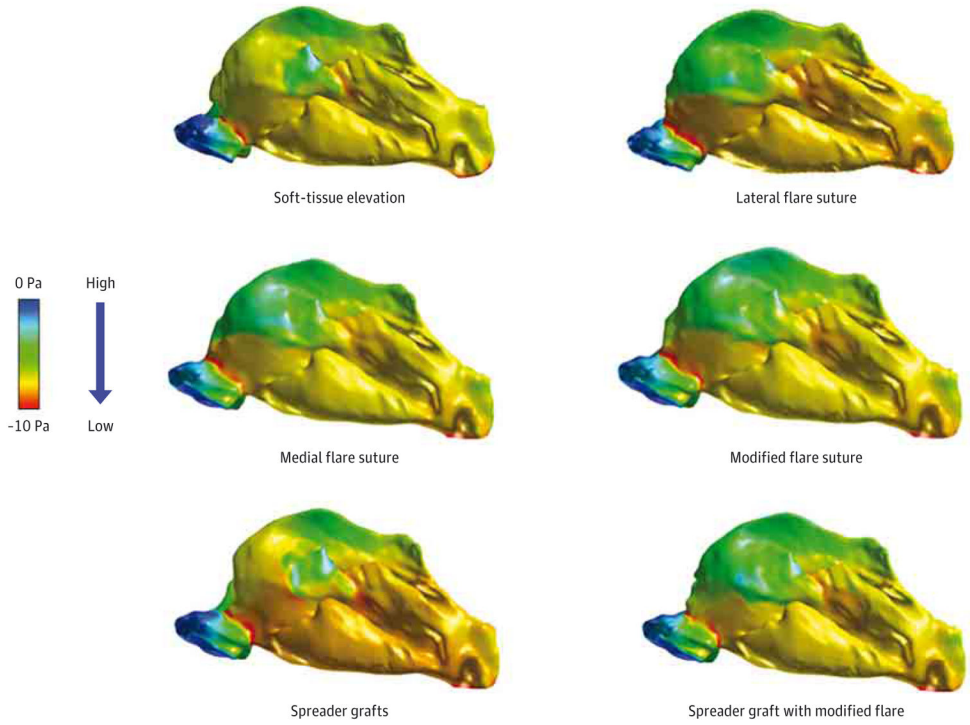

Figure 3.

Variable Pressure Gradients Along the Path of the Left Nasal Cavity

Progression from high pressure to low pressure is depicted by the color bar. The low-pressure zone of the internal nasal valve is demarcated by the red stripe seen in all models.

Author Manuscript Author Manuscript Author Manuscript Author Manuscript

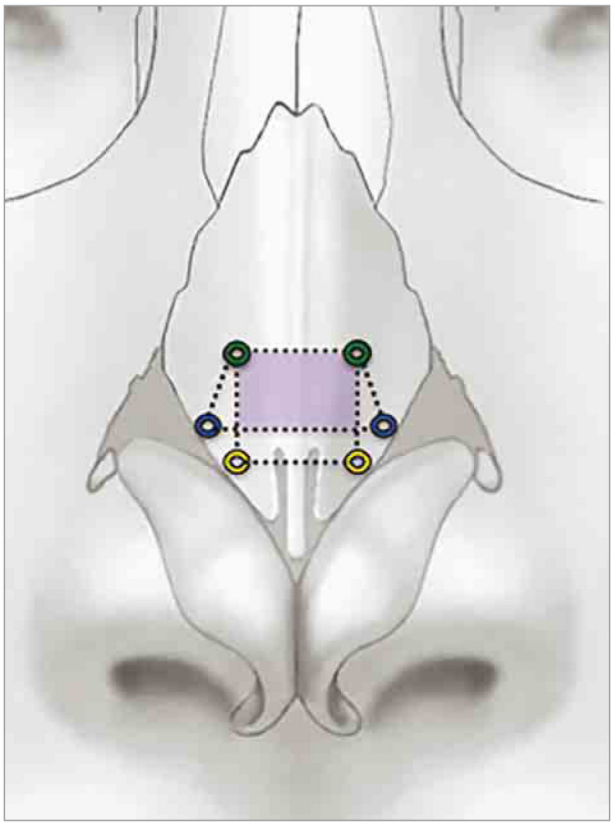

Figure 4.

Cephalic Point for Medial and Modified Flare Sutures

The medial (yellow) and modified (blue) flare sutures share the same cephalic point (green). The shaded area (purple) outlines the common critical region transformed with use of the medial or the modified flare sutures. The lateral flare suture is not pictured.

Author Manuscript

Author Manuscript

Author Manuscript

Author Manuscript

Table 1

Nasal Airflow

Model	Nasal Airflow, L/min	Increase in Airflow, %
Soft-tissue elevation	21.9	Reference
Flare suture		
Lateral	24.1	10.0
Modified	25.2	15.1
Medial	25.6	16.9
Spreader graft	23.2	5.9
Spreader graft with modified flare	24.8	13.2

Author Manuscript

Author Manuscript

Author Manuscript

Author Manuscript

Table 2

Airflow Partitioning

Model	Airflow Partitioning, %		Change in Points, %
	Left Side	Right Side	
Soft-tissue elevation	33.3	66.7	Reference
Flare suture			
Lateral	41.6	58.4	8.3
Modified	43.8	56.2	10.5
Medial	43.3	56.7	10.0
Spreader graft	39.6	60.4	6.3
Spreader graft with modified flare suture	46.1	53.9	12.8

Author Manuscript

Author Manuscript

Author Manuscript

Author Manuscript

Table 3

Bilateral Nasal Resistance

Model	Bilateral Nasal Resistance, Pa/(mL/s)	Change, %
Soft-tissue elevation	0.0205	Reference
Flare suture		
Lateral	0.0198	−3.4
Modified	0.0183	−10.7
Medial	0.0179	−12.7
Spreader graft	0.0210	2.4
Spreader graft with modified flare	0.0186	−9.3

Author Manuscript

Author Manuscript

Author Manuscript

Author Manuscript

Table 4

Unilateral Nasal Resistance

	Unilateral Resistance, Pa/(mL/s)			
Model	**Left Side**	**Change, %**	**Right Side**	**Change, %**
Soft-tissue elevation	0.0619	Reference	0.0305	Reference
Flare suture				
Lateral	0.0480	−22.5	0.0336	10.2
Modified	0.0421	−32.0	0.0322	5.6
Medial	0.0416	−32.8	0.0312	2.3
Spreader graft	0.0536	−13.4	0.0345	13.1
Spreader graft with modified flare	0.0406	−34.4	0.0341	11.8